

Wind-induced modulation of seasonal phytoplankton blooms in the North Atlantic derived from satellite observations

Rei Ueyama¹ and Bruce C. Monger

Department of Earth and Atmospheric Sciences, Cornell University, Ithaca, New York 14853

Abstract

We examined the interannual variability in the timing and magnitude of seasonal phytoplankton blooms in the North Atlantic (70°N–10°N, 90°W–10°E) in relation to variability in wind forcing during the bloom period using satellite data from 1998 through 2004. When averaged over the period extending from 1998 to 2004, seasonal increases in phytoplankton in the subpolar North Atlantic were observed predominantly during the spring, while the increases occurred between autumn and winter in the subtropical region. The major modes of interannual variability in bloom timing and magnitude from empirical orthogonal function analysis exhibited large spatial coherency across the North Atlantic. These patterns of variability can be explained, in large part, by the pattern of interannual variability in bloom-period wind mixing. Although convection is important in the seasonal development of blooms, wind-induced mixing during the bloom period appeared to be the key forcing agent contributing to interannual variability in the intensity of blooms. Increased wind-induced mixing during the bloom period reduced bloom magnitude over the subpolar and northern subtropical regions while enhancing it over the southern subtropical region. Atmospheric variations associated with interannual variability in wind mixing during the bloom period also appeared to affect variability in the timing of bloom onset. The major mode of interannual variability in the timing of North Atlantic blooms indicates a possible link to the North Atlantic Oscillation.

Phytoplankton blooms in the North Atlantic are the most pronounced of any open-ocean region (Yoder 1993; Antoine et al. 1996) and have been the focus of many studies, including Joint Global Ocean Flux Study (Koeve and Ducklow 2001) programs such as the North Atlantic Bloom Study (Ducklow and Harris 1993) and the British Ocean Flux Study (Savidge et al. 1992). Mechanisms that give rise to seasonal increases in phytoplankton were first described nearly 70 yr ago (Gran and Braarud 1935; Sverdrup 1953). However, such studies relied on data collected from research cruises, with only limited spatial and temporal resolution. The launch of ocean color satellites has since allowed oceanographers to monitor ocean productivity globally with very high resolution.

On a basin scale, bloom dynamics involve the balance

¹ Present address: Department of Atmospheric Sciences, University of Washington, Box 351640, Seattle, Washington 98195.

Acknowledgments

We thank the SeaWiFS Project Office and NASA Goddard Earth Sciences Distributed Active Archive Center for providing the chlorophyll data, Remote Sensing Systems (sponsored by the NASA Pathfinder Program) for providing the SSM/I wind speed data, and the NOAA-CIRES Climate Diagnostic Center for their NCEP/NCAR Reanalysis surface heat flux data. Charles Greene and Daniel Wilks are gratefully acknowledged for their insightful comments. We are also grateful for the thorough reviews by two anonymous referees; their constructive criticism was useful in improving the manuscript. Financial support was provided in part by the Significant Opportunities in Atmospheric Research and Science (SOARS[®]) program of the University Corporation for Atmospheric Research, with funding from the National Science Foundation, the U.S. Department of Energy, the National Oceanic and Atmospheric Administration, and Goddard Space Flight Center, NASA. This research was completed by Rei Ueyama in partial fulfillment of the requirements for the M.S. Degree Program in the Department of Earth and Atmospheric Sciences at Cornell University.

between nutrient entrainment and light limitation, regulated by the depth of the mixed layer relative to the critical depth (Sverdrup 1953). Strong convective mixing supplies nutrients to surface waters for phytoplankton growth while simultaneously limiting light availability at depths. Dutkiewicz et al. (2001) showed that vertical mixing in the upper-ocean boundary layer can increase productivity in the surface waters through enhanced nutrient supply from deep waters but can also decrease productivity due to the mixing of phytoplankton below the critical depth. In the subtropical region, increased mixing during the bloom period supplies nutrients from the deep waters to the upper ocean, where light is not limiting, thus having a positive effect on phytoplankton blooms. In the subpolar region, enhanced vertical mixing during the bloom period mixes phytoplankton below the critical depth at which light is limiting. Therefore, contrary to the subtropics, an increase in springtime vertical mixing in the subpolar North Atlantic has a negative effect on blooms (Dutkiewicz et al. 2001; Follows and Dutkiewicz 2002).

The timing of bloom onset is also of great ecological importance. Surface wind influences bloom timing via its effect on the strength and depth of vertical mixing. Stirring of the upper ocean, stimulated by the passage of weather systems during the late-winter to early-spring period, disrupts the development of water column stratification (Stramska et al. 1995) and thereby affects the timing of seasonal increases in phytoplankton. Modest light levels during late winter and early spring, combined with calm wind conditions that lead to shallow surface mixed layers, can stimulate early phytoplankton growth, prior to the development of thermal stratification (Townsend et al. 1992; Stramska and Dickey 1994). Year-to-year variations in the frequency and intensity of these mixing events are associated with atmospheric synoptic events (i.e., storms) and circulation (Dickson et al. 1996).

Moreover, surface heat flux is expected to have an indirect effect on bloom dynamics. The extent of cooling or warming of the surface waters determines the depth of the mixed layer and, consequently, light and nutrient conditions of the upper ocean. For example, strong cooling of the ocean during the winter leads to a deep end-of-winter mixed layer (Cayan 1992) that supplies nutrients to the surface waters in preparation for a possibly large spring bloom. A deep winter mixed layer may also delay springtime shoaling of the seasonal thermocline and the onset of spring blooms.

This article examines the 1998–2004 average bloom timing, bloom magnitude, bloom-period wind mixing, and winter heat flux in the North Atlantic. Spatial and temporal variability of the parameters during this time period are quantified using empirical orthogonal function (EOF) analysis. Qualitative descriptions of their patterns of variability and their relationships to one another are presented. Furthermore, since this study concerns the basin-scale variability of phytoplankton blooms in the North Atlantic on an interannual time scale, the EOF results are also discussed in relation to the North Atlantic Oscillation (NAO).

Methods

Study region and data description—Daily Standard Mapped Images (SMI) of SeaWiFS surface chlorophyll concentration (reprocessing 4) were obtained from the NASA Goddard Distributed Active Archive Center. SMI chlorophyll data were rebinned to $1^\circ \times 1^\circ$ to reduce the influence of mesoscale variability. Wind data, at a $1^\circ \times 1^\circ$ resolution, were collected daily by special sensor microwave/imager (SSM/I) instruments and scaled to 10-m surface wind speeds (Atlas et al. 1996). SSM/I data and images were produced by remote sensing systems and sponsored by the NASA Pathfinder Program for early Earth Observing System products. Daily NCEP/NCAR reanalysis surface heat flux data (Kalnay et al. 1996) were provided by the NOAA-CIRES Climate Diagnostics Center at $1.8^\circ \times 1.8^\circ$ resolution. We calculated the daily net surface heat flux over the ocean by summing daily values of net long-wave and short-wave radiation and net latent and sensible heat fluxes. Winter heat flux was computed as a 3-month (Dec–Jan–Feb) mean of the daily values. SeaWiFS data were analyzed for the period from 1 September 1997 through 24 December 2004. All other data sets were analyzed for the period from 1 September 1997 through 31 December 2004 in the region bound by 70°N – 10°N , 90°W – 10°E .

Since this study examines the different bloom responses in the subpolar and subtropical North Atlantic, a clear distinction between the two regions is needed. Zero wind stress curl contours are often used to define the subpolar and subtropical North Atlantic (Marshall et al. 2001) and were plotted on all images for reference. Henceforth, we refer to the region north of the northernmost contour as the “subpolar region” and the region bounded by the two contours in the central North Atlantic as the “subtropical region.” Wind stress curl climatology data were obtained from the Lamont–Doherty Earth Observatory Web page (updated 23 October 2003; <http://iridl.ldeo.columbia.edu/SOURCES/.TRENBERTH/>) (Trenberth et al. 1989).

Bloom period—Phytoplankton concentrations increase significantly during spring stratification in the subpolar North Atlantic. Parts of the subtropics, on the other hand, do not exhibit clearly defined blooms that are characteristic of the temperate North Atlantic as a result of relatively small seasonal variation in surface heat flux. Nonetheless, destratification of the water column during autumn enhances nutrient fluxes to surface waters and stimulate modest increases in phytoplankton in the subtropics (Yoder et al. 1993; Follows and Dutkiewicz 2002). These events are sometimes called “entrainment blooms” (Michaels 1996; McGillicuddy 2003) and are observed in the subpolar region as well, though less distinctively than are spring blooms. Indeed, Yoder and Kennelly (2003) found a 6-month phase shift in the timing of maximum phytoplankton concentration in subpolar (spring–summer peak) and subtropical (autumn–winter peak) regions. Thus, we refer to autumn or winter increases in phytoplankton as the subtropical bloom, comparable to spring or summer blooms in the subpolar North Atlantic. To account for subtropical bloom periods that may extend past January, we define each bloom year as the time period from 1 September through 31 August of the following year. For example, bloom year from 1 September 1997 through 31 August 1998 is referred to as year 1998.

The start and end days of the bloom period were determined at each $1^\circ \times 1^\circ$ location for each year (1998–2004) by analyzing a least-squares fit curve describing bloom dynamics. Fitting a least-squares curve to the annual chlorophyll time series is desirable for effectively capturing the seasonal increase in phytoplankton while eliminating high-frequency noise. Blooms can be categorized either as persistent, intense increases in phytoplankton or as longer-lasting, intermittent increases that are less intense, stimulated by the interruption of stratification following the passage of weather systems and propagation of mesoscale eddies (Stramska and Dickey 1994; Lévy et al. 2000; Waniek 2002). Attempts to fit simple functions, such as a Gaussian curve, often fail for the latter bloom type, which is characterized by multiple peaks in chlorophyll concentration during the bloom period. Hence, to be inclusive of bloom periods with large fluctuations, a more stable curve-fitting procedure was developed.

First, chlorophyll measurements were run through a three-point spatial median filter, and values greater than 30 mg m^{-3} were removed for data quality control. Second, missing chlorophyll values in the time series for a given location were filled using linear interpolation. Third, the chlorophyll time series was adjusted for each location so that the largest seasonal bloom would be at the center of its time series. To find the start and end dates of the time series for a given location, the peak chlorophyll date was first identified from a 30-point (temporal) median filtered chlorophyll time series. Then the time series was defined from a maximum of 150 d before the peak date to a maximum of 150 d after the peak date. The earliest possible start date of the time series was set to 1 September, and the latest possible end date was set to 31 August. Fourth, in a manner analogous to the running mean, the variance over a 5-d period, centered on each new day, was computed from the three-point smoothed chlorophyll time series beginning and ending on the dates specific

to each location. Five-day period was chosen as a compromise between the need for a reliable variance estimate and the desire to maintain high temporal resolution of the data. Fifth, the 5-d variances were cumulatively summed, day by day, to create a time series of the cumulative variance. Sixth, a sigmoidal curve was fit to the cumulative variance time series using a nonlinear least-squares method. The sigmoidal curve was represented as

$$f(t) = \frac{C_1}{1.0 + C_2 \times e^{-C_3 t}} + C_4$$

where t is time and C values are constants defining the shape of the fitted curve. Finally, the bloom start and end dates were functionally defined where the slope of the fitted-curve equaled one-twentieth of its maximum slope.

Typical examples of this bloom-period defining procedure at four locations in the North Atlantic are illustrated in Fig. 1. Note that the cumulative variance and fitted curves do not run through the entire time series (1 September–31 August); they are analyzed on the adjusted time series defined for that specific location, as described above in step 3. This procedure was repeated at each location in the North Atlantic for each year. The average timing of bloom onset for the period extending from 1998 to 2004 was also computed.

Bloom magnitude—The magnitude of the seasonal increase in phytoplankton is expressed as a normalized index of bloom intensity, in which the absolute magnitude of chlorophyll concentration during the bloom period is normalized relative to the average chlorophyll concentration during the nonbloom period. A normalized index of bloom intensity was chosen so that large variability over the subpolar region would not overwhelm the small but relevant variability observed in the subtropical region.

To compute the normalized bloom magnitude, chlorophyll concentrations during the bloom period at a given location for a given year were integrated and divided by the bloom duration. The average chlorophyll concentration during the nonbloom period was computed in a similar manner. The average chlorophyll concentration during the bloom period was then divided by the average nonbloom-period chlorophyll concentration. These steps were repeated at each location for each year. The average bloom magnitude for the period ranging from 1998 to 2004 was also computed.

Bloom-period wind mixing—Mixed-layer models link surface wind forcing to upper-ocean boundary-layer mixing via the generation of turbulent kinetic energy (TKE) (Kraus and Turner 1967; Niiler and Kraus 1977). Mixing by TKE is often represented as the cube of surface wind speed (u^3) multiplied by a bulk aerodynamic constant. We parameterized the wind-induced vertical mixing using just u^3 , since normalization of the data set in an EOF analysis removes the bulk constant from the wind parameter. By defining the wind-induced mixing simply as u^3 , we avoid inappropriate selection of this ambiguous bulk constant. Several studies have also parameterized the vertical turbulent mixing in this manner (Haney et al. 1981; Cayan 1992). Cubed winds were averaged during the bloom period for each year and location.

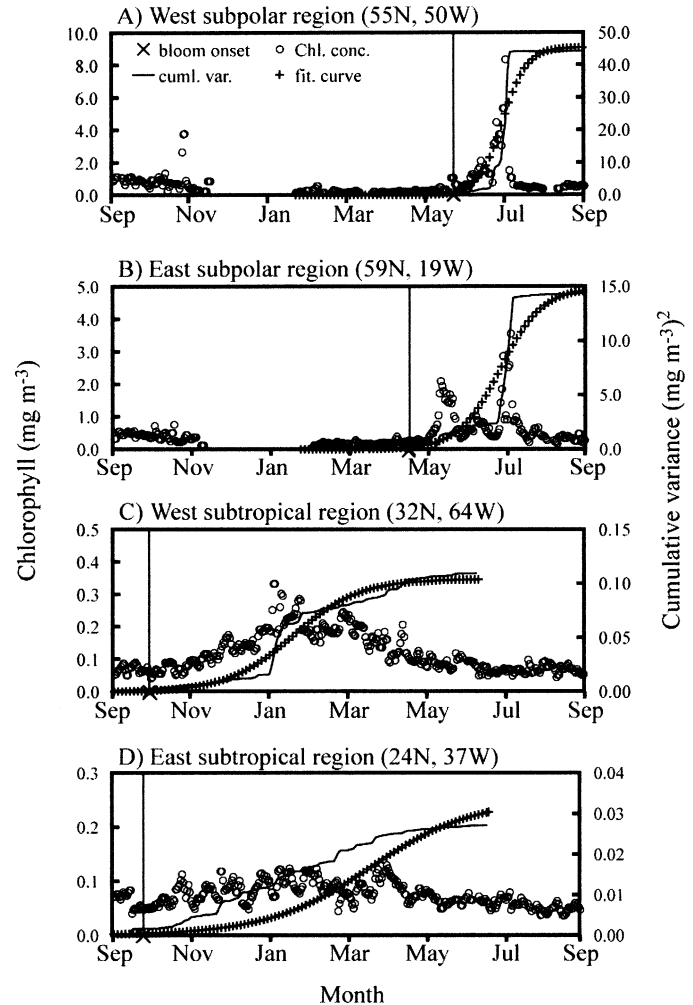


Fig. 1. 2002 time series of chlorophyll concentration, cumulative variance in chlorophyll, least-squares fit curve to the cumulative variance (solid curve with crosses), and timing of bloom onset (vertical line at X) at (A) west subpolar region, (B) east subpolar region, (C) west subtropical region, and (D) east subtropical region. Cumulative variance and its least-squares fit are analyzed on the adjusted time series (see Methods).

The 1998–2004 average bloom-period wind mixing was also computed.

EOF analysis—EOF analysis was used to examine the spatial and temporal variability of the parameters (bloom timing, bloom magnitude, bloom-period wind mixing, winter heat flux). Also known as the principal component analysis, this method is a coordinate transformation based on analysis of the covariance matrix (Wilks 1995; Emery and Thompson 1997). It reduces the dimensionality of a multivariate data set by projecting points onto a space of fewer dimensions while retaining those characteristics that contribute most of the variance. EOF is routinely used in atmospheric studies (Wallace and Gutzler 1981; Wilks 1995) as well as in physical and biological oceanography (Wilson and Adamec 2001; Yoder and Kennely 2003).

EOF analysis extracts different modes of variability into

a series of orthogonal functions. The resulting spatial eigenfunctions represent spatial patterns that vary with time, according to their corresponding principal components (PCs). Considering M yearly composites from a $(K \times 1)$ data vector x , the spatial and temporal variance of the centered (or anomaly) data, x' , can be partitioned into m modes. The original anomaly data, x'_k , can be recovered from the spatial eigenfunctions, e , that have PCs, u , using the formula

$$x'_k = \sum_{m=1}^M (e_{km}u_m), \quad k = 1, \dots, K$$

In this study, spatial eigenfunctions and their corresponding PCs were calculated using the singular value decomposition (SVD) method, since SVD is computationally more efficient and yields identical EOF results (Wilks 1995). Henceforth, we refer to SVD interchangeably as EOF.

EOF images of bloom timing, bloom magnitude, and bloom-period wind mixing are expected to be rather noisy, since the original data are themselves noisy and sparse. Another limitation is that our analyses consider only 7 yr of data. Furthermore, the EOF results—particularly the higher-order modes—may not necessarily correspond to direct physical forcing mechanisms. Despite such constraints, the time-varying spatial eigenfunctions of the leading EOF modes can be interpreted in relation to known physical processes.

Data sets were prepared in four discrete steps before applying the EOF. First, data were run through a three-point spatial median filter to reduce some noise. Second, to remove any long-term trends that may exist during the period extending from 1998 to 2004, data were temporally detrended by removing the linear trend at each $1^\circ \times 1^\circ$ bin determined by a least-squares linear fit. Third, the smoothed, detrended data sets were converted to anomaly data sets by subtracting the temporal mean at each location. Finally, with the exception of the bloom timing data set, data were normalized by dividing by their standard deviations. Normalization was done to reduce extreme events in areas of high variability (i.e., subpolar regions) relative to areas of low variability (i.e., subtropical regions), without damping the anomalies entirely. EOF analysis is only valid for a full 7-yr data set. Thus, if a given location contained missing data of a given parameter for one or more years during the 1998–2004 period, data from that location were omitted from the analysis.

EOF analyses were performed separately on bloom timing, bloom magnitude, bloom-period wind mixing, and winter heat flux data sets. Although the leading modes of all four parameters only represent about a third of each of their total variances, the spatial patterns of the second mode and the modes thereafter were less coherent, making interpretation of the results difficult. Thus, only the results of the first EOF modes are presented. PCs of the first EOF modes were correlated with PC-based indices of winter NAO during the 1998–2004 period to examine whether NAO-induced changes in the surface wind field had a discernible effect on bloom timing and magnitude. NAO Index Data were provided by the Climate Analysis Section, NCAR (Boulder, Colorado) (Hurrell 1995).

Results

Bloom timing—Seasonal increases in phytoplankton in the North Atlantic during the 1998–2004 period were observed between late September and June (Fig. 2A). With the exception of late spring to summer blooms (May–July) in the coastal regions in the southwest basin, blooms occurred between autumn and winter in subtropical regions south of 40°N . North of 40°N , blooms were observed around March. The timing of bloom onset propagated northward with time, reaching the northern subpolar regions in late May or June. These results are generally consistent with those of Yoder and Kennelly (2003).

Compared to the bloom onsets, bloom end dates were highly variable. The relative bloom magnitude parameter accounts for the uncertainty in the accuracy of bloom end dates, since the parameter places relatively little weight on the bloom duration. In general, however, bloom duration was longer in the subtropics than in the subpolar region by about 2 months (data not shown), possibly because of the long-lasting, low-intensity blooms of the subtropics (Fig. 1).

The leading EOF mode of bloom timing accounts for approximately 28% of the total variance (Figs. 2B, 3A). Early bloom onsets characterize the northern subtropics, which are in contrast with the relatively delayed bloom onsets of the surrounding regions. This pattern is most pronounced during 2000 and 2004 and is reversed in 2001 and 2003. The most noticeable feature in the second EOF mode pattern is the relatively coherent central North Atlantic region that exhibited late bloom onsets in 1998, followed by early bloom onsets in 1999 and 2000 (data not shown). The second mode accounts for about 21% of the total variance.

Bloom magnitude—Relative bloom magnitudes during the 1998–2004 period are maximal (~ 1.5 dimensionless units) in the central subtropics and decrease to the north and south of this region (Fig. 2C). We later discuss the similarity between this spatial pattern and that of the seasonal amplitude of sea-surface temperature in the North Atlantic. There is also an area of particularly high relative bloom magnitudes (>1.5) in the southwest basin, off the coast of Venezuela.

The leading EOF mode of relative bloom magnitude explains about 37% of the total variance (Figs. 2D, 3B). During positive PC years, from 1999 through 2002, the subtropical region exhibited relatively high bloom magnitudes. We note that the subtropics are divided around 25°N via a track of low bloom magnitudes orientated in the southwest to northeast direction. This quasi-latitudinal line quite accurately separates regions of different bloom response to wind forcing, as we later show. In 1999, 2000, and 2002, in particular, lower bloom magnitudes extended from 45°N to 60°N and were intersected by a region of higher bloom magnitudes at about 55°N , between Greenland and Iceland. This pattern reversed in 1998, 2003, and 2004. The second EOF mode explains about 21% of the total variance (data not shown). Quasi-latitudinal bands with alternating phases are somewhat evident in the second mode, but the data are generally noisy.

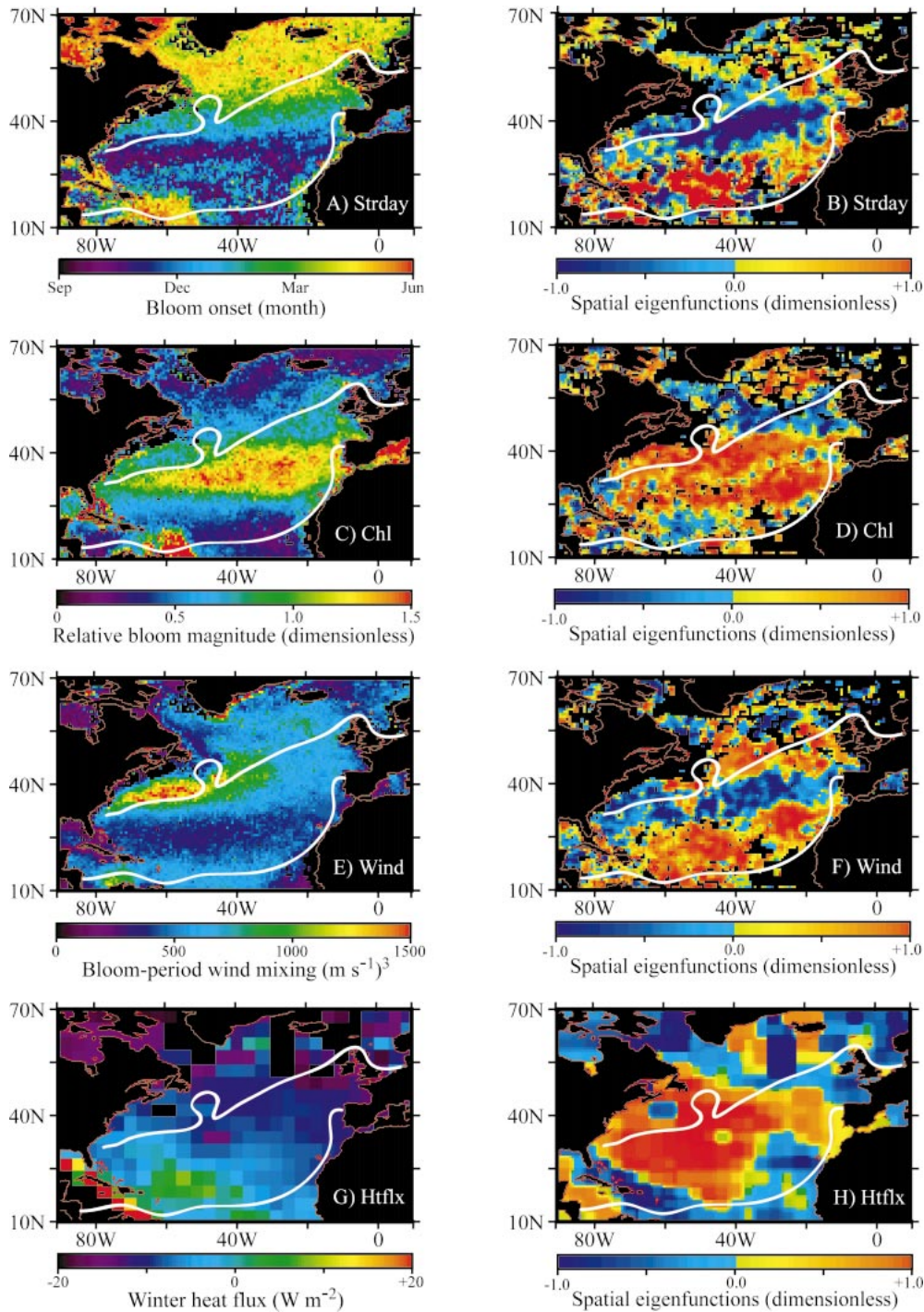


Fig. 2. 1998–2004 average (A) bloom timing—Strday, (C) relative bloom magnitude—Chl, (E) bloom-period wind mixing—Wind, and (G) winter heat flux—Htflx. Spatial eigenfunctions for the leading EOF of (B) Strday, (D) Chl, (F) Wind, and (H) Htflx during 1998–2004 account for 28%, 29%, 27%, and 31% of the total variance, respectively. Zero wind stress curl contours are overlaid on the images for reference (Trenberth et al. 1989).

Bloom-period wind mixing—The 1998–2004 period average wind mixing during the bloom period shows vigorous mixing [$1,000\text{--}1,500 (m s^{-1})^3$] in the Gulf Stream region (Fig. 2E). On the contrary, southern subtropical regions exhibited relatively low bloom-period wind mixing [$300\text{--}500$

$(m s^{-1})^3$]. Wind mixing over the remaining regions, including the subpolar and the northern and southernmost subtropical regions, was about $500\text{--}700 (m s^{-1})^3$.

The leading EOF mode of wind mixing during the bloom period explains about 27% of the total variance (Figs. 2F,

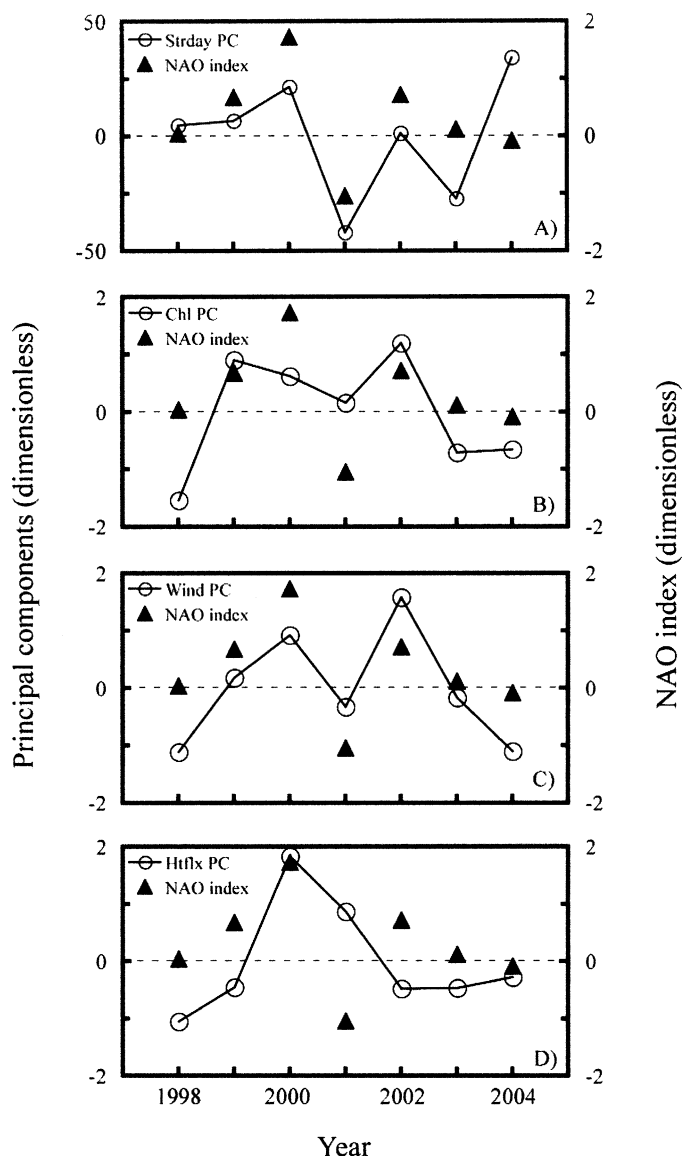


Fig. 3. Principal components (PCs) for the leading EOF of (A) bloom timing—Strday, (B) relative bloom magnitude—Chl, (C) bloom-period wind mixing—Wind, and (D) winter heat flux—Htflx overlaid with principal component-based winter (Dec–Jan–Feb–Mar) NAO index during 1998–2004 (Hurrell’s NCAR Climate Analysis Web page). The r^2 values between the principal components and the NAO indices are 0.352, 0.201, 0.397, and 0.092, respectively. The r^2 value between the principal components of relative bloom magnitude and bloom-period wind mixing is 0.740.

3C). The spatial pattern depicts alternating quasi-latitudinal bands of high and low wind mixing. With the exception of the southern subtropics, these bands correspond well with those of the leading EOF pattern of bloom magnitude (Fig. 2D), though with opposite phases. The temporal patterns (Fig. 3B,C) are also remarkably similar to each other ($r^2 = 0.740$, $p = 0.01$). During the positive PC years of 1999, 2000, and 2002, bloom-period wind mixing was high in northern subpolar and southern subtropical regions. A region of low bloom-period wind mixing in the northern subtropics

lies between these two high regions. Smaller but distinct patches of low wind mixing are also observed in the northern subpolar North Atlantic, including the region between Greenland and Iceland, at about 55°N – 65°N . This pattern reversed most evidently in 1998 and 2004. We also note that the spatial pattern of bloom-period wind mixing generally resembles that of bloom timing EOF (Figs. 2B, 3A).

The second EOF mode pattern, representing about 20% of the total variance, exhibits a fairly coherent region in the central North Atlantic (data not shown). However, the corresponding PCs hover around zero during these years, except in 2003, when the central North Atlantic experienced relatively low wind mixing.

Winter heat flux—The 1998–2004 average winter heat flux is characterized by general cooling of the ocean, with the most intense cooling in the subpolar North Atlantic ($< -10 \text{ W m}^{-2}$) (Fig. 2G). There is slight warming of the ocean (0 – 10 W m^{-2}) in the western subtropics and a maximum warming ($> 20 \text{ W m}^{-2}$) further west in the Caribbean Sea.

The leading EOF mode of winter heat flux explains about 31% of the total variance (Figs. 2H, 3D). A relatively coherent region in the central North Atlantic experienced warming of the ocean during positive PC years, 2000 and 2001. In contrast, northern and southern basins experienced cooling, with patches of warming near Greenland and Iceland and in the Caribbean Sea. This pattern reversed during 1998, 1999, 2002, 2003, and 2004. Temporal variability in the spatial pattern of winter heat flux, as depicted by its PCs, was uncorrelated with that of bloom timing ($r^2 = 0.000$, $p = 1.00$) and bloom magnitude ($r^2 = 0.167$, $p = 0.36$) (Fig. 3A,B,D).

The second EOF mode explains about 24% of the total variance (data not shown). A large coherent region across the southern North Atlantic, south of about 40°N and 25°N in the western and eastern basins, respectively, exhibited negative winter heat flux during 1999. A latitudinal band of positive winter heat flux north of this region forms a dipole structure. The phases of this dipole pattern reverse in 2000.

Discussion

The mean and major modes of interannual variability in the timing and magnitude of phytoplankton blooms in the North Atlantic have been determined from an analysis of 7 yr of satellite observations. By also presenting the major mode of variability in wind mixing and net surface heat flux over the same time period, we are able to make some inferences about the relationship between the timing and magnitude of blooms and the underlying physical forcing. In the discussion that follows, we place our observations of the mean and modal patterns of bloom timing and magnitude in the context of previous work.

Mean pattern of bloom timing—Seasonal increase of phytoplankton in the subpolar region is a consequence of the formation of thermal stratification that inhibits wind mixing below the critical depth. Timing of stratification is a function of increased solar heating in spring and may be modulated

by wind mixing during late winter to early spring (Townsend et al. 1992; Stramska et al. 1995). When averaged over many years, year-to-year variability in mixing is dampened, and the timing of thermal stratification in the subpolar region follows a general pattern of delayed stratification at higher latitudes set by increasing solar radiation input. The timing of bloom onset in the subpolar North Atlantic, as determined in the present analysis, begins around March at about 40°N and propagates northward, ending in late May at higher latitudes (Fig. 2A).

In the northern subtropical region, convective entrainment of nutrients in autumn drives the main seasonal increase in phytoplankton (Menzel and Ryther 1961; Michaels and Knap 1996; McGillicuddy et al. 2003). Consequently, the timing of bloom onset is closely tied to the reduction of solar heat flux in autumn. Using the same logic applied to spring bloom formation, the strength of wind forcing in autumn is expected to modulate the timing of bloom onset on a year-to-year basis, while the mean pattern of bloom timing is set primarily by seasonal change in solar heating. Our results indicate that the seasonal increase in phytoplankton begins in late autumn or early winter in the northern subtropics (Fig. 2A), which is consistent with the idea of an entrainment-driven increase.

In the southern subtropical region, convective supply of nutrients is negligible (Williams et al. 2000), and nutrients are supplied to the euphotic zone in roughly equal proportions by vertical advection and vertical mixing (McGillicuddy et al. 2003). Assuming a relatively constant advective component, seasonal variation in wind speed is expected to drive a seasonal change in wind mixing and, consequently, a seasonal increase in phytoplankton. Data presented by Houghton (1989) and by Servain et al. (1985) indicate that wind speeds over the western tropical Atlantic reach a minimum in late summer, begin to increase in early winter, and continue to increase into spring. The timing of bloom onset observed in the present data coincides with this seasonal increase in wind speed in early winter (Fig. 2A).

The oceanic region influenced by the Orinoco River plume shows a bloom onset date that is much later than the rest of the southern subtropical gyre (Fig. 2A). The Orinoco River discharge rate increases from March through August, stimulating early-summer phytoplankton blooms off the coast of Venezuela (Muller-Karger and Castro 1994).

Mean pattern of bloom magnitude—Phytoplankton blooms in the North Atlantic, as measured by the bloom parameter index, exhibit maximal values at midlatitude regions (Fig. 2C). This pattern arises partly from the use of the relative bloom magnitude parameter, which represents the increase in chlorophyll concentration during the bloom period relative to the average chlorophyll value during the rest of the year at a specific region. Since the mean chlorophyll concentration is highest in the subpolar North Atlantic, it is not too surprising that maximum relative magnitudes are not found there. Furthermore, this maximal region in the central subtropics corresponds to the location of maximal seasonal variability in surface heating, as reflected in the seasonal amplitude of sea–surface temperature (Cherniawsky and Oberhuber 1996). Large seasonal variability in surface

heating destabilizes the water column and enhances vertical mixing, leading to enhanced blooms in the central North Atlantic. This is consistent with the findings of Colebrook (1979) on the relationship between bloom formation and sea–surface temperature. There is also a region of large bloom magnitudes near the Orinoco River plume that is forced in a unique way by seasonal river discharge (Muller-Karger and Castro 1994) and is therefore not considered in the present article.

General remarks on interannual variability—We examined the patterns of interannual variability exhibited by the first EOF mode. As mentioned earlier, regions with spatial eigenfunctions of the same/opposite sign denote regions that change in/out of phase with each other through time. Moreover, if the principal components from separate EOF analyses have similar oscillating trends from year to year (Fig. 3), then their corresponding spatial eigenfunctions can be used to infer whether the parameters vary in phase or out of phase with one another. It is worth noting here that the principal components of bloom timing and magnitude generally resemble those of bloom-period wind mixing (Fig. 3A–C). This resemblance allows qualitative comparisons of the spatial patterns of variability in the bloom parameters and bloom-period wind mixing (Fig. 2B,F). The spatial pattern of variability in winter heat flux (Fig. 2H), however, cannot be easily interpreted in relation to the other parameters because of its unique temporal variability (Fig. 3D). Similarity in the spatial patterns of bloom magnitude and winter heat flux (Fig. 2D,H), for example, does not indicate a correlation between the two parameters because of the mismatch in their corresponding temporal patterns (Fig. 3B,D). We include EOF results of winter heat flux for the completeness of our argument. Since this study concerns the general trend of North Atlantic bloom dynamics and the underlying physical forcing, we chose a simple approach using independent EOF analyses, rather than performing an extended EOF analysis of two or more variables.

We added the zero wind stress curl contours to Fig. 2 as an obvious guide for the reader's eye. It appears that the choice of zero wind stress curl line may not be the optimal choice for delimiting the subpolar and subtropical gyres in the northeast Atlantic; in all cases, the patterns of variability tend to slope below the zero wind stress curl contour in the northeast Atlantic. Nevertheless, this criterion was retained because the well-established wind stress curl climatology data set by Trenberth et al. (1989) serves as a stable benchmark from which to examine the position of key features in the North Atlantic. For the remainder of this article, we merge the narrow region south of the zero wind stress curl line in the northeast basin with the rest of the subpolar region.

Interannual variability in bloom timing—The pattern of variability in bloom onset exhibits three primary regions (Fig. 2B): subpolar gyre and northern and southern subtropical gyres. In the subpolar gyre, reduced mixing associated with calm wind conditions over an unstratified water column in late winter can create suitable light conditions for phytoplankton growth, leading to early spring blooms (Town-

send et al. 1992; Stramska and Dickey 1994). Similarly, exceptionally stormy conditions in early spring can delay the onset of the spring bloom (Waniek 2003). The observed relationship between the strength of wind forcing and timing of bloom onset in the subpolar region is noisy (Fig. 2A,F). However, with the exception of the Labrador Sea region and a fairly broad central subpolar region (both of which may have been influenced by sea ice formation), the subpolar gyre exhibited delayed bloom onset during years of enhanced wind mixing. There are obviously other factors affecting the timing of bloom onset, most notably a variation in the net heat flux.

The subtropical gyre is clearly separated into northern and southern halves that vary out of phase from each other, as denoted by spatial eigenfunctions of the opposite sign. The relationship between interannual variability in wind forcing and the timing of seasonal increase over most of the subtropical gyre is remarkably consistent. Years of strong/weak wind mixing correspond to years of late/early timing of seasonal increases in phytoplankton (Fig. 2B,F). Although the timing of bloom onset in the northern subtropical region is mainly set by convective entrainment of nutrients in autumn, these results indicate that interannual variability in wind mixing is an important source of interannual variability in bloom timing.

We realize that interannual variability in the timing of bloom onset should be compared with interannual variability in wind mixing prior to bloom onset, rather than with variability in wind mixing during the bloom period. This may be part of the reason for the noisy relationship observed in the subpolar region. Nonetheless, it is reasonable to assume that anonymously windy conditions before the bloom onset reflect anonymously windy conditions during the early days of the bloom period. Hence, as a first-order approximation, we consider the bloom wind parameter to represent the degree of storminess throughout and prior to the onset of the bloom period.

Interannual variability of bloom magnitude—The pattern of interannual variability in bloom magnitude in the subpolar region shows a broad band of negative spatial eigenfunctions across the southern half of the subpolar region and a region of positive values further north (Fig. 2D). The pattern of variability in wind mixing is opposite to that of bloom magnitude (Fig. 2F). This out-of-phase relationship implies that strong winds have a negative impact on bloom development. Follows and Dutkiewicz (2002) recognized this remarkable feature and illustrated the positive and negative relationships of chlorophyll and wind using two scatterplots—one for the subpolar region bins and one for the southern subtropical region bins. Our results are also consistent with the argument of Dutkiewicz (2001), who claimed that vigorous wind mixing during the bloom period in light-limited regions with shallow critical depths reduces light availability, leading to diminished blooms. The weak response of phytoplankton to winter heat-flux variations in the subpolar region may be a result of the small vertical nitrate gradient at the base of the seasonal layer. When convection acts on a weak vertical gradient of nitrate, even a reasonably large change in the depth of winter convective mixing will have a small effect on the

end-of-winter nutrient concentration. Williams et al. (2000) showed that weak vertical nitrate gradient, along with modest changes in the end-of-winter mixed layer depth, causes small annual variations in convective nitrate flux at high latitudes. Since variations in winter heat flux do not appear to significantly influence springtime light or nutrient condition at high-latitude regions, it is unlikely that interannual variability in winter heat flux will force large interannual variability in spring bloom magnitude over the subpolar North Atlantic.

Bloom magnitude over much of the subtropical gyre, excluding the Orinoco River plume area, varied coherently in time (Fig. 2D). Given the bipolar pattern of variability in wind mixing (Fig. 2F), this implies that bloom magnitude is out of/in phase with wind forcing in the northern/southern subtropical gyres.

The positive relationship between bloom magnitude and wind mixing in the southern subtropical region is consistent with the idea that when light is not limiting, an increase in bloom-period wind mixing enhances nutrient input into the euphotic zone, leading to higher chlorophyll concentrations (Follows and Dutkiewicz 2002). Our observation is also consistent with that of Williams et al. (2000), who showed that the convective supply of nitrate is small across most of the subtropics south of 30°N. Furthermore, McGillicuddy et al. (2003) indicated that convective supply of nitrate to the surface layer is negligible in the permanently stratified waters of the eastern subtropics at the Eutrophic, Mesotrophic, and Oligotrophic site (21°N, 31°W) and that vertical mixing was a major contributor to total nutrient input.

In the northern subtropics, bloom magnitude is clearly out of phase with the strength of wind mixing. We expected a more ambiguous response to wind in this region because of its location between the light-limited subpolar gyre and the nutrient-limited southern subtropical gyre. Follows and Dutkiewicz (2002) had omitted this region between the subtropical and subpolar “regimes” in their discussion of bloom and wind. Moreover, we expected to see a close correspondence between interannual variations in bloom magnitude and winter heat flux based on previous documentation of the relationship between interannual variability in primary production and chlorophyll biomass, with variability in the depth of winter convection (Menzel and Ryther 1961; Michaels and Knap 1996). However, this connection was not observed in the present data (Fig. 2D,H).

The spatial pattern of winter heat flux variability in the subtropics (Fig. 2H) coincides with the centers of anomalies of air–sea heat fluxes and sea surface temperature tendencies (Cayan 1992). However, variability in winter heat flux exhibits little or no relationship to variability in bloom magnitude because of the uncorrelated temporal patterns of the two (Fig. 3B,D). The accuracy of the surface heat flux estimates from the NCEP/NCAR reanalysis is not well constrained (Kistler et al. 2001; Moore and Renfrew 2002). Nonetheless, given the assumption that these products depict actual heat flux values to a reasonable degree, our results indicate that interannual variations in bloom-period wind mixing had a larger impact on the interannual variability in bloom magnitude than did interannual variations in winter heat flux during the 1998–2004 period. With mixed layer

depths typically exceeding 200 m during the entrainment period (Steinberg et al. 2001), enhanced wind mixing during this period is expected to reduce light availability and diminish bloom magnitude, as was evident in our observations.

NAO-related patterns of bloom variability—EOF analyses performed in this study have revealed that major modes of interannual variability in bloom timing and magnitude are related to the major mode of variability in wind mixing during the bloom period. Since the major mode of wind variability in the North Atlantic is associated with the NAO (Visbeck et al. 2001), we briefly explored the connection between interannual variability in the bloom parameters and the NAO index.

Phytoplankton variability in the North Atlantic and its relationship with the NAO have been examined in the past (Reid et al. 1998; Barton et al. 2003). Follows and Dutkiewicz (2002) showed that increased nutrient flux to surface waters associated with enhanced winter mixing in the subtropics—a characteristic of negative NAO condition—is an important source of interannual variability in phytoplankton biomass and productivity. EOF results by Yoder and Kennelly (2003) indicated that the effects of NAO are detectable as interannual chlorophyll anomalies in analyses focusing on northern hemisphere middle- to high-latitude basins. When we correlated the first principal component of bloom magnitude with the principal component-based winter (Dec–Jan–Feb–Mar) NAO index, we found the relationship insignificant ($r^2 = 0.20$) (Fig. 3B). The correlation between the first principal component of bloom onset and the principal component-based NAO index (Fig. 3A), however, was somewhat stronger ($r^2 = 0.35$). This implies that winter NAO conditions may set the stage for bloom initiation. However, the link between bloom timing and NAO is still speculative at the present time. Future studies should investigate whether this relationship will hold on a decadal or longer time scale.

Observations of the major modes of variability in bloom magnitude and wind forcing are consistent with previous results by Follows and Dutkiewicz (2002). Building upon their pioneering work, our EOF results provide a basin-scale view of the year-to-year variability in bloom timing, bloom magnitude, wind mixing, and winter heat flux in high spatial resolution during the 1998–2004 period. In addition to the remarkable spatial coherency of bloom and wind variability observed in our results, this approach revealed an important contribution of wind mixing to bloom variability in the northern subtropical gyre, a region omitted in the study by Follows and Dutkiewicz (2002). Interannual variability in bloom magnitude in this region has always been linked to variability in deep convective mixing associated with heat loss beginning in early winter. Given that mixed layers during the bloom period in the northern subtropical gyre often exceed 200 m, it is perhaps not too surprising that winds are able to modulate bloom magnitudes. While NAO-related effects may have influenced the timing of bloom onset during 1998–2004, future work is needed to examine the relationship between bloom magnitude and net surface heat flux to better assess the effects of climate variability on phytoplankton dynamics and ecosystem response.

References

- ANTOINE, D., J. M. ANDRE, AND A. MOREL. 1996. Ocean primary production 0.2. Estimation at global scale from satellite (coastal zone color scanner) chlorophyll. *Global Biogeochem. Cycles* **10**: 57–69.
- ATLAS, R., R. HOFFMAN, S. BLOOM, J. JUSEM, AND J. ARDIZZONE. 1996. A multi-year global surface wind velocity data set using SSM/I wind observations. *Bull. Am. Meteorol. Soc.* **77**: 869–882.
- BARTON, A. D., C. H. GREENE, B. C. MONGER, AND A. J. PERSHING. 2003. The Continuous Plankton Recorder survey and the North Atlantic Oscillation: Interannual- to multidecadal-scale patterns of phytoplankton variability in the North Atlantic Ocean. *Prog. Oceanogr.* **58**: 337–358.
- CAYAN, D. R. 1992. Latent and sensible heat flux anomalies over the northern oceans: Driving the sea surface temperature. *J. Phys. Oceanogr.* **22**: 859–881.
- CHERNAIAWSKY, J. W., AND J. M. OBERHUBER. 1996. The seasonal cycle of mixed layer temperatures in a global ocean general circulation model. *Climate Dynamics* **12**: 171–183.
- COLEBROOK, J. M. 1979. Continuous plankton records: Seasonal cycles of phytoplankton and copepods in the North Atlantic Ocean and the North Sea. *Mar. Biol.* **51**: 23–32.
- DICKSON, R. R., J. LAZIER, J. MEINCKE, P. RHINES, AND J. SWIFT. 1996. Long-term coordinated changes in the convective activity of the North Atlantic. *Prog. Oceanogr.* **38**: 241–295.
- DUCKLOW, H. W., AND R. P. HARRIS. 1993. Introduction to the JGOFS North Atlantic bloom experiment. *Deep-Sea Res. II* **40**: 1–8.
- DUTKIEWICZ, S., M. FOLLOWS, J. MARSHALL, AND W. W. GREGG. 2001. Interannual variability of phytoplankton abundances in the North Atlantic. *Deep-Sea Res. II* **48**: 2323–2344.
- EMERY, W. J., AND R. E. THOMPSON. 1997. Data analysis methods in physical oceanography. Pergamon.
- FOLLOWS, M., AND S. DUTKIEWICZ. 2002. Meteorological modulation of the North Atlantic spring bloom. *Deep-Sea Res. II* **49**: 321–344.
- GRAN, H. H., AND T. BRAARUD. 1935. A quantitative study of the phytoplankton on the Bay of Fundy and the Gulf of Maine. *J. Biol. Board Can.* **1**: 279–433.
- HANEY, R. L., M. S. RISCH, AND G. C. HEISE. 1981. Wind forcing due to synoptic storm activity over the North Pacific Ocean. *Atmos. Ocean* **19**: 128–147.
- HOUGHTON, R. W. 1989. Influence of local and remote wind forcing in the Gulf of Guinea. *J. Geophys. Res.* **94**: 4816–4828.
- HURRELL, J. W. 1995. Decadal trends in the North Atlantic Oscillation: Regional temperatures and precipitation. *Science* **269**: 676–679.
- KALNAY, E., AND OTHERS. 1996. The NCEP/NCAR 40-year reanalysis project. *Bull. Am. Meteorol. Soc.* **77**: 437–471.
- KISTLER, R., AND OTHERS. 2001. The NCEP-NCAR 50-year reanalysis: Monthly means CD-ROM and documentation. *Bull. Am. Meteorol. Soc.* **82**: 247–267.
- KOEVE, W., AND H. W. DUCKLOW. 2001. JGOFS synthesis and modeling: The North Atlantic Ocean. *Deep-Sea Res. II* **48**: 2141–2154.
- KRAUS, E. B., AND J. S. TURNER. 1967. A one-dimensional model of the seasonal thermocline. Part II: The general theory and its consequences. *Tellus* **19**: 98–106.
- LÉVY, M., L. MÉMERY, AND G. MADEC. 2000. Combined effects of mesoscale processes and atmospheric high-frequency variability on the spring bloom in the MEDOC area. *Deep-Sea Res. I* **47**: 27–53.
- MARSHALL, J., H. JOHNSON, AND J. GOODMAN. 2001. A study of

- the interaction of the North Atlantic Oscillation with ocean circulation. *J. Climate* **14**: 1399–1421.
- MCGILLICUDDY, D. J., JR., L. A. ANDERSON, S. C. DONEY, AND M. E. MALTRUD. 2003. Eddy-driven sources and sinks of nutrients in the upper ocean: Results from a 0.1° resolution model of the North Atlantic. *Global Biogeochem. Cycles* **17**: 1035–1054.
- MENZEL, D. W., AND J. H. RYTHER. 1961. Annual variations in primary production in the Sargasso Sea off Bermuda. *Deep-Sea Res.* **I 7**: 282–288.
- MICHAELS, A. F., AND A. H. KNAP. 1996. Overview of the U.S. JGOFS Bermuda Atlantic time-series Study and the Hydrostation S program. *Deep-Sea Res.* **II 43**: 157–198.
- MICHAELS, A., AND OTHERS. 1996. Inputs, losses and transformations of nitrogen and phosphorus in the pelagic North Atlantic Ocean. *Biogeochemistry* **35**: 181–226.
- MOORE, G. W. K., AND I. A. RENFREW. 2002. An assessment of the surface turbulent heat fluxes from the NCEP-NCAR reanalysis over the western boundary currents. *J. Climate* **15**: 2020–2037.
- MULLER-KARGER, F. E., AND R. A. CASTRO. 1994. Mesoscale processes affecting phytoplankton abundance in the southern Caribbean Sea. *Cont. Shelf Res.* **14**: 199–221.
- NIILER, P. P., AND E. B. KRAUS. 1977. One-dimensional models of the upper ocean, p. 143–172. *In* E. B. Kraus [ed.], *Modeling and prediction of the upper layers of the ocean*. Pergamon.
- REID, P. C., M. EDWARDS, H. G. HUNT, AND A. J. WARNER. 1998. Phytoplankton change in the North Atlantic. *Nature* **391**: 546.
- smSavidge, G., and others. 1992. The BOFS 1990 spring bloom experiment: Temporal evolution and spatial variability of the hydrographic field. *Prog. Oceanogr.* **29**: 235–281.
- SERVAIN, J., J. PICAUT, AND A. J. BUSALACCHI. 1985. Interannual and seasonal variability of the tropical Atlantic Ocean depicted by sixteen years of sea-surface temperature and wind stress, p. 211–237. *In* J. C. J. Nihoul [ed.], *Coupled ocean-atmosphere models*. Elsevier.
- STEINBERG, D. K., C. A. CARLSON, N. R. BATES, R. J. JOHNSON, A. F. MICHAELS, AND A. H. KNAP. 2001. Overview of the US JGOFS Bermuda Atlantic Time-series Study (BATS): A decade-scale look at ocean biology and biogeochemistry. *Deep-Sea Res.* **II 48**: 1405–1447.
- STRAMSKA, M., AND T. D. DICKEY. 1994. Modeling phytoplankton dynamics in the northeast Atlantic during the initiation of the spring bloom. *J. Geophys. Res.* **99**: 10241–10253.
- , ———, A. PLUEDDERMANN, R. WELLER, C. LANGDON, AND J. MARRA. 1995. Bio-optical variability associated with phytoplankton dynamics in the North Atlantic ocean during spring and summer of 1991. *J. Geophys. Res.* **100**: 6621–6632.
- SVERDRUP, H. U. 1953. On conditions for the vernal blooming of phytoplankton. *J. Cons. Int. Explor. Mer* **18**: 287–295.
- TOWNSEND, D. W., M. D. KELLER, M. E. SIERACKI, AND S. G. ACKLESON. 1992. Spring phytoplankton blooms in the absence of vertical water column stratification. *Nature* **360**: 59–62.
- TRENBERTH, K., J. OLSON, AND W. LARGE. 1989. A global ocean wind stress climatology based on ECMWF analyses. National Center for Atmospheric Research, Boulder, Colorado.
- VISBECK, M. H., J. W. HURRELL, L. POLVANI, AND H. M. CULLEN. 2001. The North Atlantic Oscillation: Past, present, and future. *Proc. Natl. Acad. Sci. USA* **98**: 12876–12877.
- WALLACE, J. M., AND D. S. GUTZLER. 1981. Teleconnections in the geopotential height field during the Northern Hemisphere winter. *Mon. Weather. Rev.* **109**: 784–812.
- WANIEK, J. J. 2003. The role of physical forcing in initiation of spring blooms in the northeast Atlantic. *J. Mar. Sys.* **39**: 57–82.
- WILKS, D. S. 1995. *Statistical methods in the atmospheric sciences*. Academic.
- WILLIAMS, R. G., AND M. J. FOLLOWS. 1998. The Ekman transfer of nutrients and maintenance of new production over the North Atlantic. *Deep-Sea Res.* **I 45**: 461–489.
- , A. J. MCLAREN, AND M. J. FOLLOWS. 2000. Estimating the convective supply of nitrate and implied variability in export production over the North Atlantic. *Global Biogeochem. Cycles* **14**: 1299–1313.
- WILSON, C., AND D. ADAMEC. 2001. Correlations between surface chlorophyll and sea surface height in the tropical Pacific during the 1997–1999 El Niño–Southern Oscillation event. *J. Geophys. Res.* **106**: 31175–31188.
- YODER, J. A., AND M. A. KENNELLY. 2003. Seasonal and ENSO variability in global ocean phytoplankton chlorophyll derived from 4 years of SeaWiFS measurements. *Global Biogeochem. Cycles* **17**: 1112.
- , C. R. MCCLAIN, G. C. FELDMAN, AND W. E. ESAIAS. 1993. Annual cycles of phytoplankton chlorophyll concentrations in the global ocean—a satellite view. *Global Biogeochem. Cycles* **7**: 181–193.

Received: 20 August 2004

Amended: 8 July 2005

Accepted: 25 July 2005